A respiratory *Streptococcus* strain inhibits *Acinetobacter* baumannii from causing inflammatory damage through ferroptosis

Ye Sun[1], Shuyin Li[1], Yuchen Che[1], Hao Liang[1], Yi Guo[2] and Chunling Xiao[1*]

Abstract

Background Microecological equilibrium is essential for human health. Previous research has demonstrated that *Streptococcus* strain A, the main bacterial group in the respiratory tract, can suppress harmful microbes and protect the body. In this study, *Streptococcus* strain D19[T] was isolated from the oral and pharyngeal cavities of healthy children. Its antibacterial mechanism against *Acinetobacter* baumannii was examined, as well as its potential to prevent inflammatory damage to cells. We evaluated the effect of the fermentation conditions of D19[T] on inhibition of *Acinetobacter* baumannii growth; Isolation and purification of antibacterial active components of strain D19[T] and molecular mechanism of inhibition of *Acinetobacter* baumannii; Molecular mechanism of D19[T] antibacterial protein reversing cellular inflammatory injury induced by *Acinetobacter* baumannii.

Results The supernatant of fermentation broth of *Streptococcus* D19[T] was the active component against *Acinetobacter* baumannii, but the bacteria had no antibacterial activity. The supernatant of D19[T] fermentation broth was precipitated by $(NH_4)_2SO_4$ solution, and the protein was the active antibacterial component. After gel filtration chromatography and anion gel filtration chromatography, the molecular weight of antibacterial protein was 53kD. D19[T] antibacterial protein can improve cell membrane permeability, limit extracellular soluble protein release, inhibit *Acinetobacter* baumannii biofilm formation, and prevent *Acinetobacter* baumannii adhesion. *Acinetobacter* baumannii induces inflammatory damage to respiratory cells via ferroptosis, and the D19[T] antibacterial protein can counteract this damage, protecting the respiratory tract.

Conclusion *Streptococcus* strain D19[T], as a potential probiotic, inhibits the growth of *Acinetobacter* baumannii and the inflammatory damage of respiratory cells, playing a protective role in human respiratory health.

Keywords *Streptococcus* strain, *Acinetobacter* baumannii, Antibacterial, Ferroptosis, Inflammation

*Correspondence:
Chunling Xiao
xiaochunling@symc.edu.cn
[1]Key Lab of Environmental Pollution and Microecology of Liaoning
Province, Shenyang Medical College, 146 Huanghe North Street, Yuhong
District, Shenyang 110034, China
[2]School of Health Management, Shenyang Vocational and Technical
College, 32 Laodong Road, Dadong District, Shenyang 110045, China

Sun *et al. BMC Microbiology*   (2024) 24:437

Page 2 of 12

Background

Human body contains billions of microbes that serve critical roles in digestion and absorption, vitamin production, immunity, and metabolism [1, 2]. The microbial community has created a symbiotic relationship with the human body, and microecology must be stable in order to preserve physical health. However, several adverse variables, such as environmental pollution, hospital infections, antibiotic usage, excessive cleaning, and improper food habits, disrupt the microbial community, resulting in a variety of health issues [3–5].

Multidrug-resistant *Acinetobacter* baumannii infections have emerged as a major hospital infection pathogen as a result of antibiotic overuse, placing a significant strain on international healthcare systems [6]. The two primary ways that *Acinetobacter* baumannii spreads are through hospital infections and community transmission [7]. *Acinetobacter* baumannii infections in hospitals have the ability to adhere to the surfaces of medical personnel, equipment, and ward items, so spreading the illness to more patients [8–10]. *Acinetobacter* baumannii mostly affects the elderly and physically frail populations, increasing the death rate of patients through a variety of routes that induce respiratory inflammation and damage. The term "dominant microbial communities" describes the microbial populations that are predominant in a particular host or environment and are crucial to preserving the microecological equilibrium. In the respiratory system, for instance, type A hemolytic *Streptococcus* strain can fend off the adhesion and invasion of pathogens like *Pseudomonas aeruginosa*, *Escherichia coli*, and *Staphylococcus aureus*, helping to keep the microbiota in the body in balance [11–13]. There is currently no information available regarding the connection between *Acinetobacter* baumannii-induced inflammation and type A hemolytic *Streptococcus* strain. The purpose of this study is to investigate *Streptococcus* strain D19^T as a dominant microbial community in the respiratory tract, analyze its anti-inflammatory effects on pathogenic bacteria, and lay the foundation for the clinical development of probiotics.

Results

Streptococcus strain D19^T inhibited the growth of *Acinetobacter* baumannii

As shown in Fig. 1-A, both *Streptococcus* strain D19^T fermentation broth and supernatant could inhibit the growth of *Acinetobacter* baumannii, but neither live or inactivated bacteria of D19^T could inhibit the growth of *Acinetobacter* baumannii. Therefore, we speculated that the supernatant of fermentation broth of strain D19^T was the active antibacterial component of *Acinetobacter* baumannii. In addition, we also optimized the fermentation conditions of strain D19^T. When the pH value of the culture medium was 7.0, the fermentation temperature was 37℃, and the fermentation time was 24 h, the supernatant of the fermentation liquid of strain D19^T obtained the greatest antibacterial effect, and the diameter of its inhibitory *Acinetobacter* baumannii was 22.09±21 mm (Fig. 1-B, C, D).

D19^T antibacterial components identification and purification

D19^T fermentation broth was centrifuged to remove bacteria to obtain the supernatant, adding $(NH_4)_2SO_4$ solution of different saturation to obtain the supernatant and precipitation. As shown in Fig. 2-A, the supernatant after the salting out of $(NH_4)_2SO_4$ solution of different saturation has no antibacterial activity, while the precipitation after the salting out of $(NH_4)_2SO_4$ solution of 30%~70% saturation has antibacterial activity. $(NH_4)_2SO_4$ solution saturation of 50% had the strongest antibacterial activity. The fermentation supernatant was precipitated with 50% saturated $(NH_4)_2SO_4$ solution and redissolved in buffer. After dialysis, the protein samples were loaded on Sephadex G-15 chromatography resin. As shown in Fig. 2-B and C, a total of three protein detection peaks appeared in the elution curve. Each protein peak was tested for activity against *Acinetobacter* baumannii, and it can be seen that protein peak a has antibacterial activity. Peak a was dialyzed and purified by anion-exchange chromatography. Three peaks were collected again after chromatography. Peak b showed antibacterial activity and a single protein band with a molecular weight of 53 KD was determined by SDS-PAGE electrophoresis (Fig. 2-D, E, F).

D19^T entered a stable growth phase at 18 h and commenced the production of antibacterial proteins. By 24 h, the levels of the antibacterial protein peaked (Fig. 2-G). The antibacterial activity exhibited by the antibacterial protein was sustained for five days at 37 °C, with no statistically significant difference observed between the antibacterial protein and the culture supernatant (Fig. 2-H). Low concentrations of salt did not affect antibacterial properties of the antibacterial protein; however, a significant reduction in their efficacy was noted at salt concentrations exceeding 0.2 mol/L (Fig. 2-I).

D19^T antibacterial protein's inhibition mechanism against *Acinetobacter* baumannii

The minimum inhibitory concentration (MIC) of D19^T was determined to be 15 mg/mL. Then, *Acinetobacter* baumannii extravasated DNA and RNA levels increased significantly at D19^T antibacterial protein concentrations ≥1/2MIC, as measured by the protein gel imaging system ($p < 0.05$) (Fig. 3-A). In addition, we also found that the soluble protein expression of *Acinetobacter* baumannii was significantly reduced at the concentration of D19^T antibacterial protein ≥1/2MIC ($p < 0.05$) (Fig. 3-B).
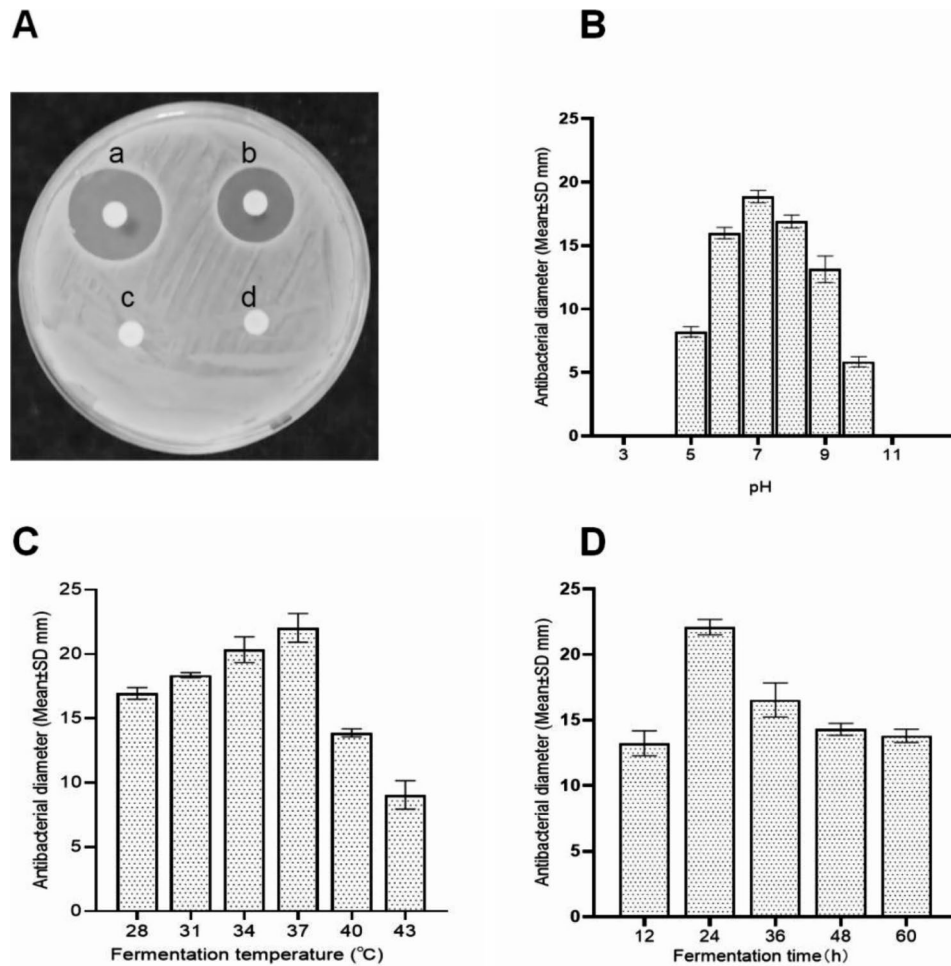
Fig. 1 D19[T] fermentation broth antibacterial assay and optimization of fermentation conditions. (**A**) Detection of antibacterial components in D19[T] fermentation broth. (**B**) Effect of fermentation broth pH on the bacteriostasis of D19[T]. (**C**) Effect of fermentation temperature on the bacteriostasis of D19[T]. (**D**) Effect of fermentation time on the bacteriostasis of D19[T]. (a) Fermentation broth. (b) Fermentation broth supernatant. (c) Live bacterial body. (d) Inactivated bacterial body

Finally, we found that *Acinetobacter* baumannii's biofilm formation and adhesion were significantly reduced at the concentration of D19[T] antibacterial protein≥1/2MIC ($p < 0.05$) (Fig. 3-C and D).

Acinetobacter baumannii induces ferroptosis in respiratory epithelial cells

Human bronchial epithelial cells BEAS-2B and 16HBE were infected with *Acinetobacter* baumannii. The ferroptosis of BEAS-2B and 16HBE cells was detected. As shown in Fig. 4-A, BEAS-2B and 16HBE cells infected with *Acinetobacter* baumannii showed significant decreases in the expression of ferroptosis-related regulatory proteins GPX4, SLC7A11, and SLC3A2 ($p < 0.05$). In addition, Fluorescence microscopy revealed that *Acinetobacter* baumannii infected BEAS-2B and 16HBE cells have increased ferroptosis fluorescence signals (Fig. 4-B).

Acinetobacter baumannii causes inflammatory damage to respiratory epithelial cells

Previous studies have confirmed that ferroptosis is closely related to inflammation, so we further studied the inflammatory damage of cells after *Acinetobacter* baumannii infection. As shown in Fig. 5-A to C, expressions of inflammatory factors TNF-α, IL-6 and IL-8 were significantly increased in BEAS-2B and 16HBE cells infected with *Acinetobacter* baumannii. ($p < 0.05$). In addition, we also examined the expression of intracellular regulatory proteins of inflammatory factors. As shown in Fig. 5-D, the expression levels of NF-κB, ASCL4, COX2 and LOX proteins were significantly increased in BEAS-2B and 16HBE cells infected with *Acinetobacter* baumannii ($p < 0.05$).
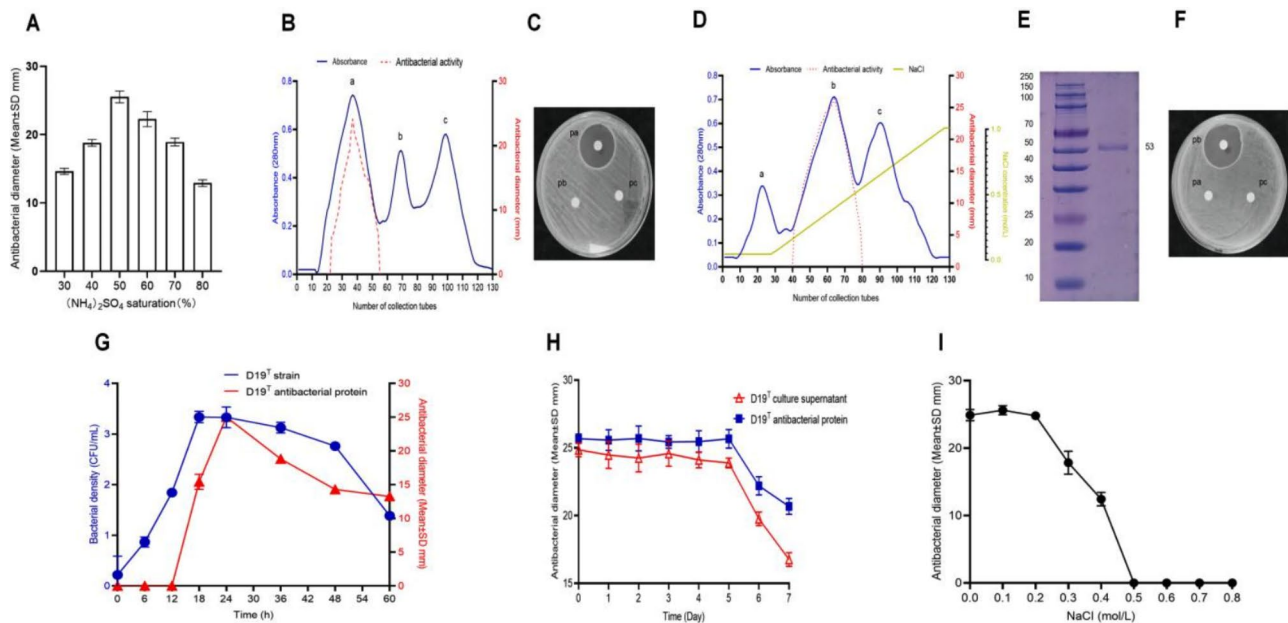
Sun *et al. BMC Microbiology*   (2024) 24:437

Page 4 of 12

Fig. 2 Isolation and purification of antibacterial active components of D19^T. (**A**) Antibacterial test of fermentation broth supernatant precipitated by $(NH_4)_2SO_4$ at different saturation. (**B**) Sephadex G-15 molecular sieve was used to isolate and purify the protein and to detect its antibacterial activity. (**C**) Antibacterial activity was detected by disk dispersion method. (**D**) Isolation and purification of protein by cellulose DE-52 chromatography and antibacterial detection. (**E**) Molecular weight determination of antibacterial protein. (**F**) Antibacterial activity was detected by disk dispersion method. (**G**) D19^T growth and production of antibacterial protein activity curve. (**H**) Culture medium supernatant and antibacterial protein activity detection at 37 °C. (**I**) Salt concentration against antibacterial protein activity detection. p.a.: peak a, pb peak b, pc peak c

D19^T antibacterial protein reverses the ferroptosis of respiratory epithelial cells induced by *Acinetobacter baumannii*

The effect of D19^T antibacterial protein on the ferroptosis of BEAS-2B and 16HBE cells infected with *Acinetobacter* baumannii was analyzed in vitro. As shown in Fig. 6-A, D19^T antibacterial protein could inhibit the ferroptosis of BEAS-2B and 16HBE cells caused by *Acinetobacter* baumannii in a concentration-dependent manner. When the concentration of antibacterial protein was ≥1/2MIC, the expression levels of ferroptosis-related regulatory proteins GPX4, SLC7A11 and SLC3A2 were significantly increased ($p < 0.05$). In addition, when the concentration of antibacterial protein was ≥1/2MIC, the intensity of intracellular ferroptosis fluorescence signals were significantly decreased in *Acinetobacter* baumannii infected BEAS-2B and 16HBE cells ($p < 0.05$)(Fig. 6-B). By electron microscopy, the antibacterial protein could restore the damage caused by Acinetobacter baumannii, such as the decrease of mitochondria, the increase of membrane density and the decrease of mitochondrial ridge(Fig. 6-C).

D19^T antibacterial protein reverses the inflammatory injury of respiratory epithelial cells induced by *Acinetobacter baumannii*

Similarly, we also analyzed the effect of D19^T antibacterial protein on inflammatory factors in BEAS-2B and 16HBE cells infected with *Acinetobacter* baumannii. As shown in Fig. 7-A to C, D19^T antibacterial protein could inhibit the inflammatory damage of BEAS-2B and 16HBE cells caused by *Acinetobacter* baumannii in a concentration-dependent manner. When the concentration of D19^T antibacterial protein was ≥1/2MIC, the expression levels of TNF-α, IL-6 and IL-8 were significantly inhibited ($p < 0.05$). In addition, the expression levels of NF-κB, ASCL4, COX2 and LOX proteins in *Acinetobacter* baumannii infected BEAS-2B and 16HBE cells were significantly decreased when the concentration of D19^T antibacterial protein was ≥1/2MIC ($p < 0.05$)(Fig. 7-D).

Discussion

Acinetobacter baumannii is an opportunistic pathogen with strong adhesion, which is a common pathogen of nosocomial infection. According to statistics, infections caused by *Acinetobacter* baumannii account for about 2% of all health care-associated infections in the United States and Europe, while the rate is significantly higher in Asia [14]. *Acinetobacter* baumannii is mainly distributed in ICU and respiratory departments of hospitals, and the objects of infection are mainly immunocompromised people, critically ill patients caused by invasive procedures, and patients treated with broad-spectrum antibiotics [15]. *Acinetobacter* baumannii mainly causes respiratory tract infection, and complications include
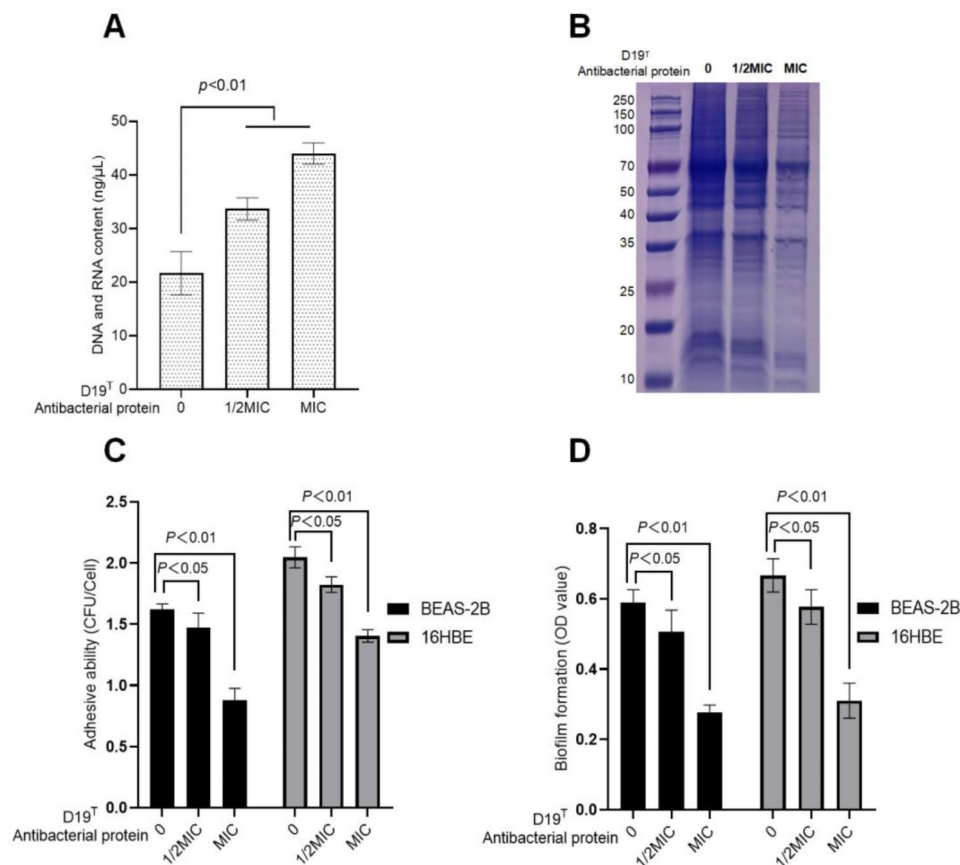
Fig. 3 Mechanism of D19^T antibacterial protein inhibiting the growth of *Acinetobacter* baumannii. (**A**) Effect of D19^T antibacterial protein on *Acinetobacter* baumannii DNA and RNA extravasation. (**B**) Effect of D19^T antibacterial protein on soluble proteins of *Acinetobacter* baumannii. (**C**) Effect of D19^T antibacterial protein on adhesion of *Acinetobacter* baumannii. (**D**) Effect of D19^T antibacterial protein on *Acinetobacter* baumannii biofilm

bacteremia, urinary tract infection, meningitis, and ventilator-associated pneumonia [16].

Biofilm refers to the bacteria secretes aggregated membrane-like substances such as polysaccharide matrix, fibrin, and lipid proteins to enclose the whole bacterial community [17]. Biofilms can resist the antibacterial effects of antibiotics, immune-clearing cells, and immune effector substances. Biofilm is the main pathogenic factor and an important antibacterial index of *Acinetobacter* baumannii. In this study, we initially confirmed the inhibitory effect of the D19^T mixture on *Acinetobacter* baumannii through antibacterial experiments. Subsequently, we isolated the fermented bacterial broth and assessed the antibacterial activity of each fraction. The results indicated that neither live nor inactivated D19^T cells exhibited any inhibitory effect on *Acinetobacter* baumannii; however, the supernatant obtained after cell removal demonstrated significant inhibitory activity against this pathogen. We then proceeded to separate and purify both protein components and other chemical constituents using ammonium sulfate precipitation followed by gel chromatography. Notably, a specific protein within the D19^T fermentation broth was identified as being active

against *Acinetobacter* baumannii. We investigated the biological characteristics of this antibacterial protein and discovered that it was produced during the stable growth phase of D19^T, with optimal inhibitory effects observed at 24 h post-cultivation. Furthermore, we found that the antibacterial activity of this protein could be sustained for up to five days at 37 °C. While variations in salt concentration within the antibacterial protein solution did not enhance its antimicrobial efficacy, an increase in salt concentration adversely affected its activity. Consequently, purified D19^T protein underwent dialysis to eliminate excess salt prior to further analysis. We also found that D19^T antibacterial protein increased the extravasation of macromolecules such as DNA and RNA in *Acinetobacter* baumannii broth. This suggests that the D19^T antibacterial protein affects the stability of *Acinetobacter* baumannii cell membrane and increases its permeability. In addition, we found that the D19^T antibacterial protein was able to inhibit the secretion of soluble proteins and reduce the efflux of toxic substances from *Acinetobacter* baumannii. Finally, our results showed that D19^T antibacterial protein significantly inhibited the biofilm formation and adhesion ability of *Acinetobacter* baumannii.
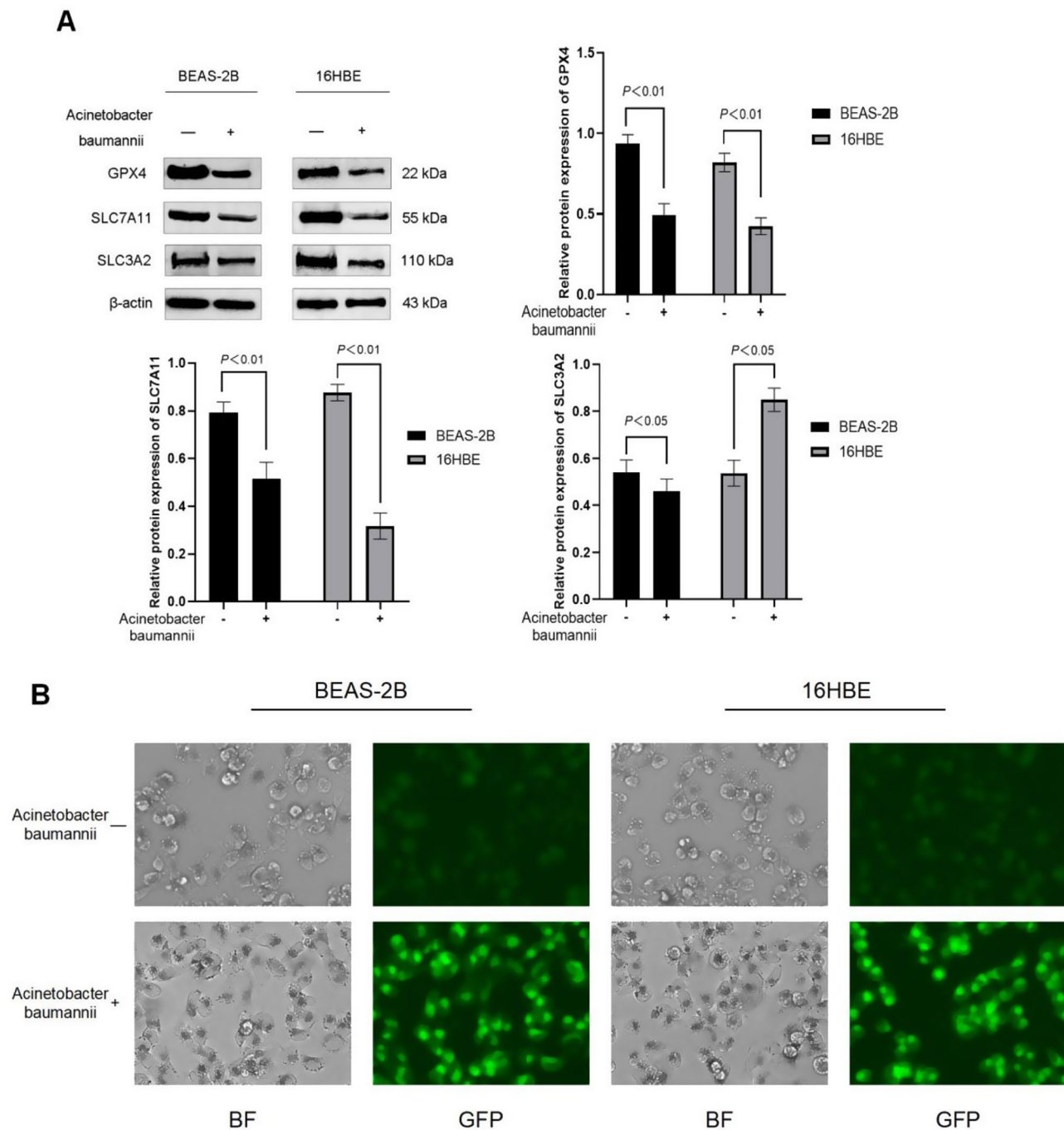
Fig. 4 *Acinetobacter* baumannii induces ferroptosis in respiratory epithelial cells. (**A**) Western blot detection of iron death related regulatory proteins. (**B**) Fluorescence labeling method to detect iron cell death. Full-length gels are presented in Supplementary Figures S1 and S2

Ferroptosis is an iron-dependent, non-apoptotic form of cell death accompanied by increased glutathione peroxidase activity and lipid peroxidation [18]. It has been confirmed that ferroptosis is closely related to the occurrence and development of many diseases, such as tumor, neurodegenerative diseases, ischemia-reperfusion injury, and so on [19]. Recent studies have found that the process of ferroptosis is often accompanied by inflammatory manifestations. When cells undergo ferroptosis, inflammation-related molecules are produced to stimulate the innate immune system, and immune cells trigger inflammatory responses by producing cytokines [20]. Lipoxygenase and epoxidation products play an important role in inflammatory response and may be closely related to ferroptosis. Our results show that *Acinetobacter* baumannii can cause inflammatory injury in human respiratory
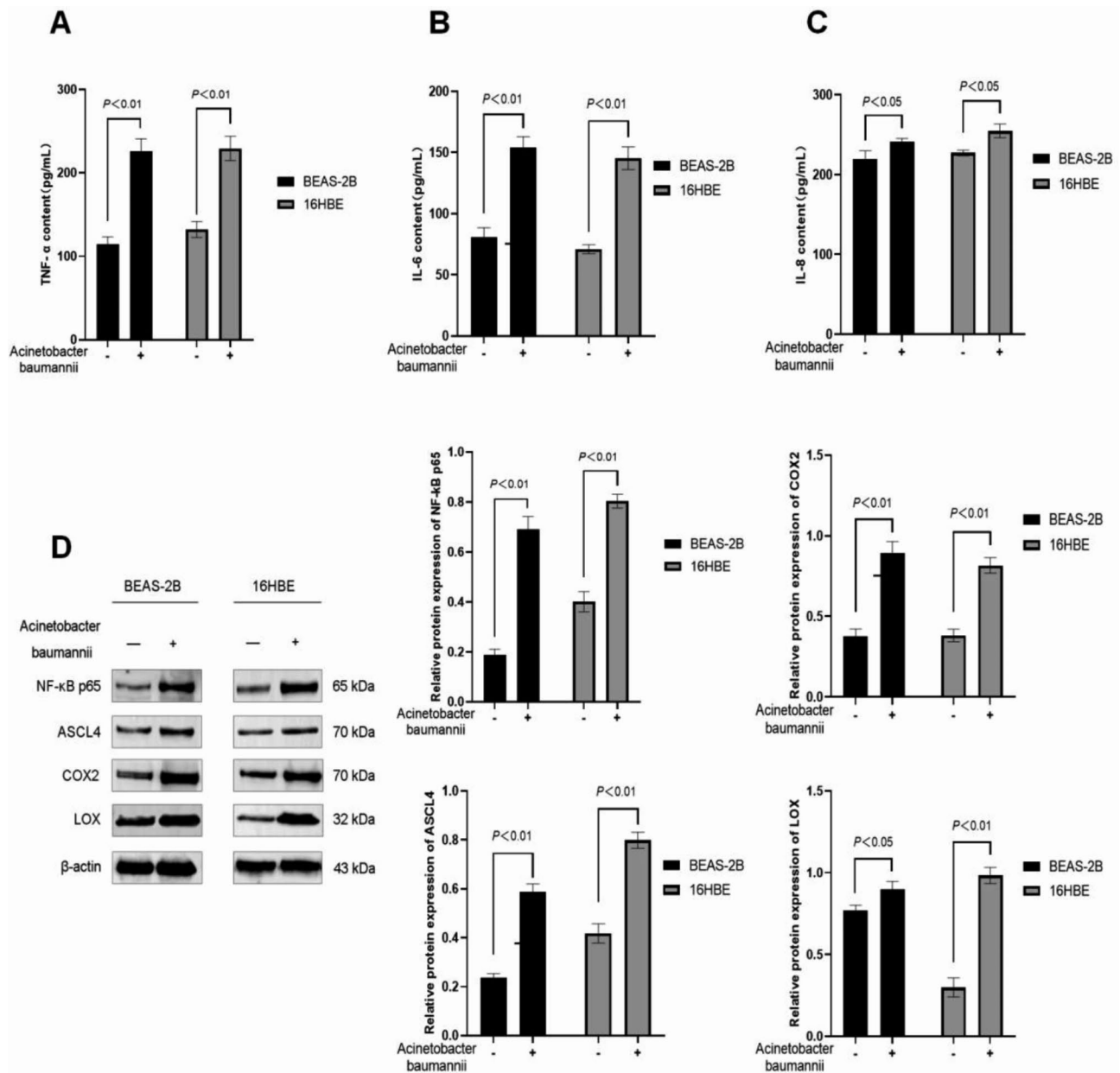
Fig. 5 *Acinetobacter* baumannii induces inflammatory injury of respiratory epithelial cells. ELISA method to detect the (**A**) TNF-α, (**B**) IL-6, (**C**) IL-8 levels. (**D**) Western blot detection of inflammatory injury related regulatory proteins. Full-length gels are presented in Supplementary Figures S3 and S4

epithelial cells through ferroptosis pathway. D19^T antibacterial protein inhibits *Acinetobacter* baumannii induced ferroptosis in respiratory epithelial cells BEAS-2B and 16HBE by up-regulating GPX4, SLC7A11 and SLC3A2 protein expression. We also found that D19^T antibacterial protein inhibited the expression of TNF-α, IL-6 and IL-8 in *Acinetobacter* baumannii infected BEAS-2B and 16HBE cells. These results suggest that D19^T antibacterial protein can reverse the inflammatory injury of respiratory epithelial cells induced by *Acinetobacter* baumannii.

In this study, we confirmed that D19^T, as the dominant bacteria in the normal human respiratory tract, could be used as a microecological agent for clinical treatment and prevention of *Acinetobacter* baumannii infection in the future. Although we have successfully isolated and purified the bacteriostatic protein from D19^T fermentation broth, the biological characteristics of the protein, such as amino acid composition, spatial conformation and active site, need to be further explored.
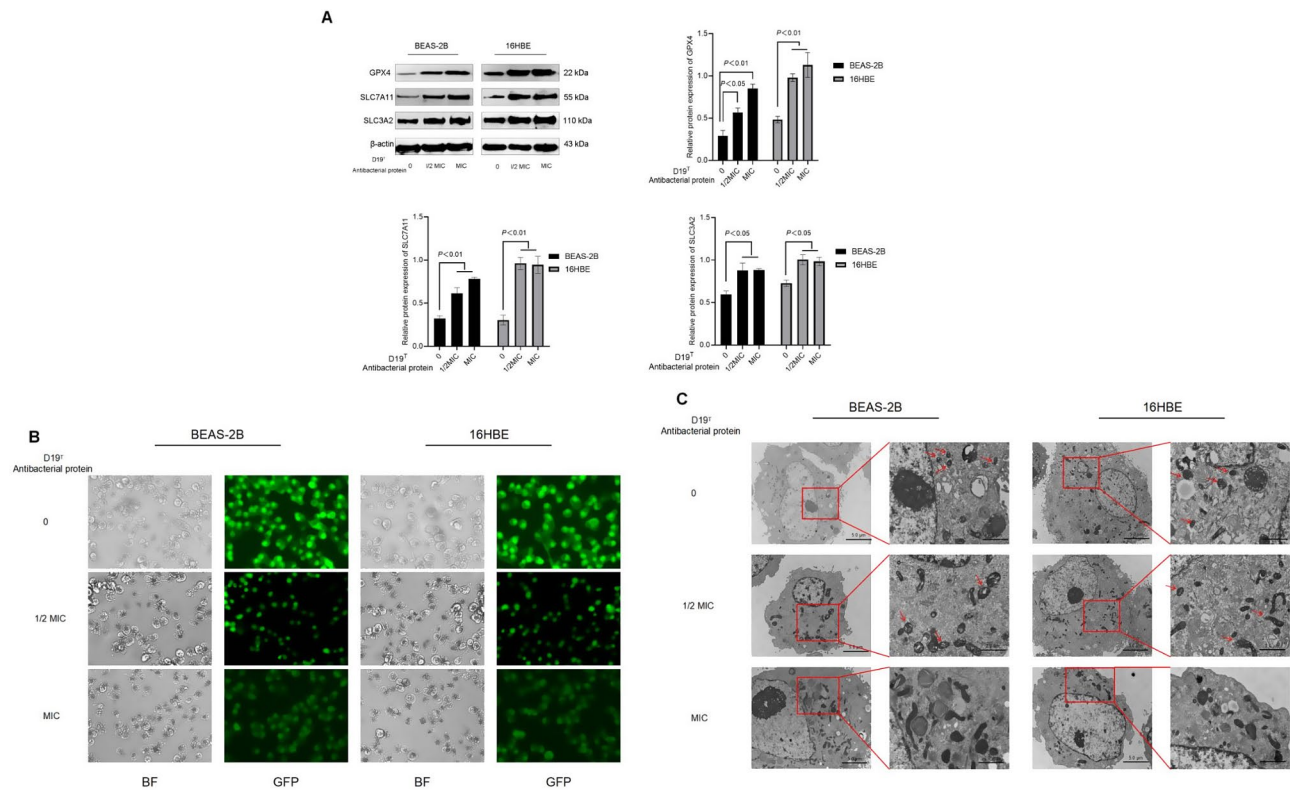
Fig. 6 Effect of D19[T] antibacterial protein on ferroptosis of respiratory epithelial cells induced by *Acinetobacter* baumannii. (**A**) Western blot detection of iron death related regulatory proteins. (**B**) Fluorescence labeling method to detect iron cell death. (**C**) Transmission electron microscopy method to detect iron cell death. Full-length gels are presented in Supplementary Figures S5 and S6

Conclusions

Acinetobacter baumannii is an important pathogen of nosocomial infection. It causes inflammatory damage to the respiratory tract through ferroptosis. *Streptococcus* strain D19[T] is the dominant bacteria in human respiratory tract colonization, which can inhibit the growth of *Acinetobacter* baumannii and reverse inflammatory damage, and play a protective role in human respiratory system health.

Materials and methods

Antibodies

The primary antibodies include mouse monoclonal anti-GPX4 (1:3000, Cat No. 67763-1-Ig), rabbit polyclonal anti-SLC7A11 (1:1000, Cat No. 26864-1-AP), rabbit polyclonal anti-SLC3A2 (1:20000, Cat No. 15193-1-AP), mouse monoclonal anti-NF-κB p65 (1:1000, Cat No. 66535-1-Ig), rabbit polyclonal anti-ASCL4 (1:6000, Cat No. 22401-1-AP), rabbit polyclonal anti-COX2 (1:2000, Cat No. 12375-1-AP), rabbit polyclonal anti-LOX (1:600, Cat No. 17958-1-AP)(Proteintech Group Inc., Rosemont, IL, USA), goat anti-rabbit IgG (1:50000, H+L, Cat No. RGAR001), and goat anti-mouse IgG (1:20000, H+L, Cat No. RGAM001) were purchased from Proteintech Group, Inc (Rosemont, IL, USA),

Strains and cells and their culture

Streptococcus strain D19[T] was collected from the oropharynx of healthy children and cultured in bacto brain heart infusion medium(Solarbio, Beijing, China) at 37 ℃, 180 r/min, for 18 h. *Acinetobacter* baumannii S2009-4 originates from the Laboratory of Shenyang Medical University Affiliated Central Hospital and is cultured in broth medium(Solarbio, Beijing, China) under conditions at 37 ℃, 180 r/min, for 18 h.

Human bronchial epithelium BEAS-2B cells and 16HBE cells were purchased from Beijing Dingguo Changsheng Biotechnology Co., LTD. BEAS-2B and 16HBE cells were cultured in DMEM(Hyclone, Logan, UT, USA) medium containing 10% fetal bovine serum(Hyclone, Logan, UT, USA), 100 units/mL penicillin(Genview, Australia), and 100 units/mL streptomycin solution(Genview, Australia) at 37 ℃ and 5% CO_2.

Antibacterial assay

The concentration of *Acinetobacter* baumannii bacterial solution in the logarithmic phase was adjusted to 1×10^6 CFU/mL, and 100 µL was removed and evenly spread on nutrient AGAR plates. Using the disk diffusion method, 200 µL of the sample solution to be tested was added to the disk and placed in a bacterial incubator for 18 h at
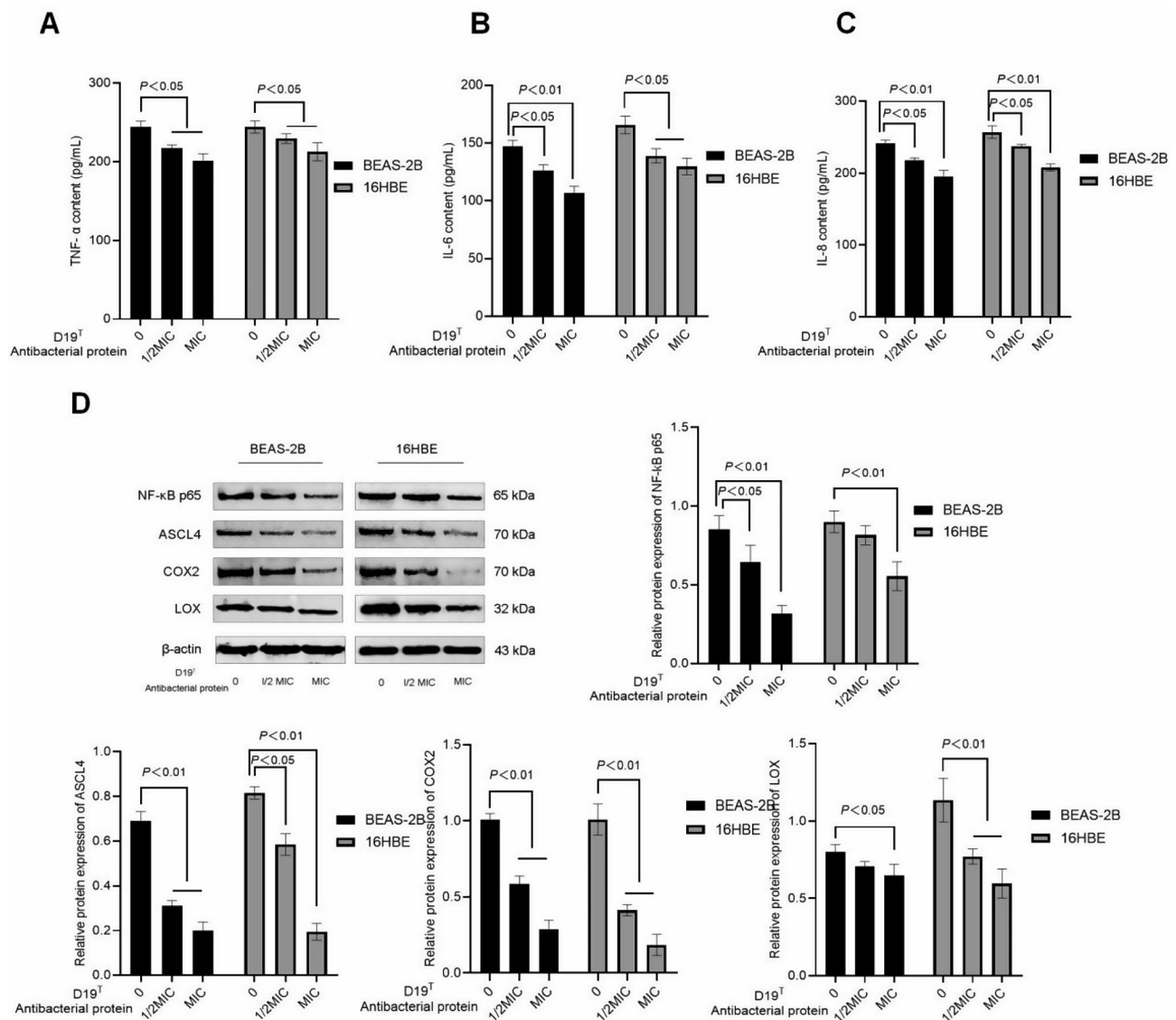
Fig. 7 Effect of D19[T] antibacterial protein on inflammatory injury of respiratory epithelial cells induced by *Acinetobacter* baumannii. ELISA method to detect the (**A**) TNF-α, (**B**) IL-6, (**C**) IL-8 levels. (**D**) Western blot detection of inflammatory injury related regulatory proteins. Full-length gels are presented in Supplementary Figures S7 and S8

37 °C. The diameter of inhibition was recorded with a vernier caliper.

Fermentation broth conditions determination

D19[T] single colonies were inoculated into brain heart infusion medium and incubated at 37 °C, 180 r/min, for 18 h. The inhibitory diameter was measured under different fermentation conditions with different pH (3–11), fermentation temperature (28–43 °C) and fermentation time (12–60 h).

Antibacterial components determination

Antibacterial component determination: D19[T] fermentation broth was centrifuged at 4 °C and 12,000 r/min for 10 min to remove bacterial cells and obtain the supernatant of the fermentation broth. Add $(NH_4)_2SO_4$ solution to the supernatant to a saturation of 30%, and precipitate overnight at 4 °C. The next day, the fermentation broth was centrifuged at 12,000 r/min for 10 min. The protein precipitate was dissolved in 50 mmol/L phosphate buffer and desalinated using a dialysis bag(Yeasen Biotechnology, Shanghai, China). Measure the antibacterial effects of the precipitated protein and supernatant separately.

The determination of the optimal concentration of $(NH_4)_2SO_4$: The method for obtaining the supernatant of D19[T] fermentation broth is consistent with the method mentioned earlier. Add $(NH_4)_2SO_4$ solution to the supernatant, and the saturation of $(NH_4)_2SO_4$ in the final supernatant ranges from 20 to 80%. Precipitate overnight

at 4 ℃. The next day, the fermentation broth was centrifuged at 12,000 r/min for 10 min. The protein precipitate was dissolved in 50 mmol/L phosphate buffer and desalinated using a dialysis bag. Measure the antibacterial effect of proteins precipitated with different saturation levels $(NH_4)_2SO_4$ separately.

Antibacterial proteins isolation and purification

The protein solution was loaded on a Sephadex G-15(Sigma, Louis, MO, USA) column and eluted with PBS solution at a flow rate of 1.5 mL/min. The elution peaks of each protein were detected and collected under ultraviolet light at 280 nm to determine the inhibitory diameter. The antibacterial active fractions were collected and concentrated and then processed by cellulose DE-52 chromatography(Biosharp, Anhui, China). The flow rate was 1.5 mL/min and equilibrated in PBS solution until the baseline was stable. Linear gradient elution was carried out with $0 \sim 1.0$ mol/L NaCL in PBS buffer, and the flow rate was controlled at 0.5 mL/min. The elution peaks of each protein were collected to determine the inhibitory diameter.

Minimum inhibitory concentration (MIC) determination

The antibacterial protein was diluted to 2, 4, 8, 16, 32 and 64 times with bacto brain heart infusion medium. 100 μL protein solution was added to 96-well plate, and 10 μL pathogen solution (1×10^6 CFU/mL) was added to each well. After mixing, the 96-well plate was cultured in a bacterial incubator at 37 ℃ for 24 h. The minimum drug concentration without bacterial growth was read by the plate viable bacteria count method, which was the minimum inhibitory concentration (MIC) of the bacteria to the drug.

DNA and RNA exosmosis levels determination

DNA and RNA exosmosis levels of *Acinetobacter* baumannii were measured using Thremo Nanodrop 2000 detector(Thermo Fisher Scientific, Waltham, MA, USA). The operation procedure is summarized as follows: Run the Nanodrop when the sample measuring arm is off, add 2 μL of distilled water to the optical fiber surface, lower the measuring arm, and set to zero. Add 1.0 μL of the sample to be measured successively, and repeat the measurement for each sample to be measured 3 times.

Soluble protein levels determination

The level of soluble protein in *Acinetobacter* baumannii was determined by SDS-PAGE. The operation steps are summarized as follows: the suspension of *Acinetobacter* baumannii after treatment in the control group and the experimental group was centrifuge and the supernatant was removed to collect the bacteria. *Acinetobacter* baumannii in each group of samples were washed with

pre-cooled PBS solution twice, the supernatant was removed by centrifuge and the bacteria were collected, then re-suspended in PBS solution and adjusted to the same bacterial density. The bacteria were treated in a metal bath at 100 ℃ for 10 min, mixed upside down once every 2 min, and the lysed cells released soluble proteins. Protein samples of 20 μL were added for SDS-PAGE electrophoresis, dyed with Coomassie bright blue (Beyotime Biotechnology, Shanghai, China) for 40 min, decolorized with distilled water, and photographed for analysis of protein expression.

Biofilm formation determination

100 μL *Acinetobacter* baumannii solution at a concentration of 1×10^6 CFU/mL was added to 96-well plate, and then antibacterial protein solution was added to the final concentration of 0, 1/2MIC and MIC, respectively, and cultured at 37 ℃ for 24 h. The culture medium and non-adherent bacteria were washed with PBS buffer, methanol was fixed for 15 min, the biofilm was stained with 2% crystal violet solution for 15 min, and the cells were decolorized with 33% glacial acetic acid. The absorbance was determined at 630 nm. The broth medium without bacteria was used as a negative control.

Adhesion ability determination

500 μL of BEAS-2B and 16-HBE cells at a concentration of 5×10^4 cells /mL were seeded onto cell slides in 6-well plates and incubated in at 37 ℃ and 5% CO_2 overnight. The cells were first cultured in serum-containing DMEM for 3 days, and then starved in serum-free DMEM culture for 12 h. After washing with PBS, 1 mL of *Acinetobacter* Baumannii suspensions with a concentration of 1×10^8 CFU/mL were added to each well, and 1mL of DMEM culture solution was added, mixed evenly, and incubated together for 2 h. The cells were washed with PBS and fixed with 4% paraformaldehyde for 30 min. The number of *Acinetobacter* baumannii adherens on the cell surface was observed and counted under the microscope. Non-adhesive bacteria (≤40 bacteria), adhesive bacteria (41–100 bacteria), strongly adhesive bacteria (>100 bacteria).

Cell iron death determination

500 μL of BEAS-2B and 16-HBE cells at a concentration of 5×10^4 cells /mL were seeded onto cell slides in 6-well plates and incubated in at 37 ℃ and 5% CO_2 overnight. Add 500 μL DMEM containing ammonium ferric sulfate (II) into each well (the final concentration of ammonium ferric sulfate (II) is 100 mol/L), and incubate in the incubator for 30 min. After washing the cells with PBS, the cells were fixed with 4% paraformaldehyde at room temperature for 30 min, and then treated with 1% Triton X-100 for 20 min. The cells were washed with PBS and

incubated in an incubator with 500 μL FerroGreen solution for 30 min. The intensity of each fluorescence signal was detected by GFP filter and BF filter in fluorescence microscope.

Inflammatory cytokines detection

The supernatant was obtained by centrifugation at 1000 g for 20 min. Standard and sample holes were set up according to TNF-α, IL-6 and IL-8 instructions(Mibio, Shanghai, China). Add 50 μL of standard product with different concentration to the standard product hole, and add 50 μL of sample to the sample hole. Horseradish peroxidase (HRP) labeled detection antibody 100 μL was added to each well and incubated in an incubator at 37 ℃ for 60 min. Add 300 μL washing solution to each well and repeat washing for 5 times. Add 50 μL of substrate A and substrate B to each well and incubate at 37 ℃ for 15 min without light. The absorbance of each hole was measured at 450 nm wavelength by adding 50 μL terminating solution to each hole.

Western blot

Wash the cells once with a pre-cooled PBS solution to remove as much excess fluid as possible. 500 μL RIPA lysate(Beyotime Biotechnology, Shanghai, China) containing 1mM PMSF(Beyotime Biotechnology, Shanghai, China) was added to the cells, and the entire lysate process was performed on ice. The protein samples were separated by SDS-PAGE gel electrophoresis at 80 V, 20 min, 120 V, 50 min. The protein on the gel was transferred to the PVDF membrane(Millipore, Boston, MA, USA) by wet transfer method at 300 mA for 2 h. The transferred PVDF film was washed with TBST and sealed overnight with 5% skim milk(Sigma, Louis, MO, USA) powder solution at 4 ℃. On the second day, they were incubated at room temperature for 1 h with first antibody diluent and second antibody diluent, respectively. The protein was developed with enhanced ECL chemiluminescence reagent (Vazyme, Shanghai, China), and the gray values of the protein bands were calculated by Image J software.

Ferroptosis was detected by electron microscopy

Cells were collected and added to the fixative precooled at 4 °C and placed at 4 °C overnight. The fixative was decanted, rinsed with phosphate buffer, and samples were fixed with 1% osmic acid solution for 2 h. The samples were dehydrated with gradient concentrations of ethanol (30%, 50%, 70%, 80%, 90%, 95%, and 100%) and finally treated with acetone. The samples were embedded in the embedding agent and cut by a microtome. The sections were stained with lead citrate solution and 50% ethanol saturated solution of uranyl acetate for 10 min, respectively, and observed under a transmission electron microscope.

Statistical analysis

Since each experiment was performed three times, the data is given as mean±SD. A two-tailed Student's t-test was used to assess the differences between the two groups. Analysis of Variance (ANOVA) is used to assess differences between multiple sets of data. P value lower than 0.05 was considered significant. SPSS 19.0 was used to analyze the data.

Abbreviations

pH	Potential of hydrogen
SDS-PAGE	Sodium dodecyl sulfate polyacrylamide gel electrophoresis
MIC	Minimum inhibitory concentration
TNF-α	Tumor necrosis factor-α
IL	Interleukin
NF-κB	Nuclear factor kappa-B
ASCL4	Achaete-scute family bHLH transcription factor 4
COX2	Cyclooxygenase-2
LOX	Lectin-type oxidized LDL receptor 1
GPX4	Glutathione peroxidase 4
SLC7A11	Solute carrier family 7, member 11
SLC3A2	Solute carrier family 3, member 3
ICU	Intensive Care Unit
PBS	Phosphate-buffered saline

Supplementary Information

The online version contains supplementary material available at https://doi.org/10.1186/s12866-024-03589-7.

Supplementary Material 1

Author contributions

CX: Experimental design (lead); funding support (lead). YS: Experimental operation (lead); data analysis (lead); article writing (lead). SL: Experimental design. YC: Experimental operation. HL: Experimental design. YG: Data analysis.

Data availability

All data included in this study are available on request from the corresponding author.

Declarations

Ethical approval

The experimental protocol was established, according to the ethical guidelines of the Helsinki Declaration and was approved by the Human Ethics Committee of Shenyang Medical College.

Consent for publication

Not applicable.

Informed consent

Written informed consent was obtained from individual or guardian participants.

Competing interests

The authors declare no competing interests.

References

1. Guo XY, Liu XJ, Hao JY. Gut microbiota in ulcerative colitis: insights on pathogenesis and treatment. J Dig Dis. 2020;21(3):147–59.
2. Fu Q, Song T, Ma X, et al. Research progress on the relationship between intestinal microecology and intestinal bowel disease. Anim Model Exp Med. 2022;5(4):297–310.
3. Wang J, Liang J, He M, et al. Chinese expert consensus on intestinal microecology and management of digestive tract complications related to tumor treatment (version 2022). J Cancer Res Ther. 2022;18(7):1835–44.
4. Isolauri E. Microbiota and obesity. Nestle Nutr Inst Workshop Ser. 2017;88:95–105.
5. Tennyson CA, Friedman G. Microecology, obesity, and probiotics. Curr Opin Endocrinol Diabetes Obes. 2008;15(5):422–7.
6. Lee CR, Lee JH, Park M, et al. Biology of *Acinetobacter* baumannii: Pathogenesis, Antibiotic Resistance mechanisms, and prospective treatment options. Front Cell Infect Microbiol. 2017;7:55.
7. Giamarellou H, Antoniadou A, Kanellakopoulou K. *Acinetobacter* baumannii: a universal threat to public health? Int J Antimicrob Agents. 2008;32(2):106–19.
8. Palethorpe S, Farrow JM, Wells G, et al. *Acinetobacter* baumregulatesuitsestressSresponsesponses via the twoRcomponentponent Regulatory System. J Bacteriol. 2022;204(2):e0049421.
9. Ramirez MS, Bonomo RA, Tolmasky ME. Carbapenemases: transforming *Acinetobacter* baumannii into a yet more dangerous menace. Biomolecules. 2020;10(5):720–50.
10. Yang CH, Su PW, Moi SH, et al. Biofilm formation in *Acinetobacter* Baumannii: genotype-phenotype correlation. Molecules. 2019;24(10):1849.
11. Zhang WX, Xiao CL. *Streptococcus* strain D19T as a probiotic candidate to modulate oral health. BMC Microbiol. 2023;23(1):339–46.
12. Liu D, Xiao C, Li X, et al. *Streptococcus* shenyangsis sp. nov., speciespisolatedolated from the Oropharynxhealthyechild Child from Shenyang China. Curr Microbiol. 2021;78(7):2821–7.
13. Qi H, Liu D, Zou Y, et al. Description and genomic characterization of *Streptococcus* symci sp. nov., isolated from a child's oropharynx. Antonie Van Leeuwenhoek. 2021;114(2):113–27.
14. AlAmri AM, AlQurayan AM, Sebastian T, et al. Molecular Surveillance of Multidrug-Resistant *Acinetobacter* baumannii. Curr Microbiol. 2020;77(3):335–42.
15. Tuan Anh N, Nga TVT, Tuan HM, et al. Molecular epidemiology and antimicrobial resistance phenotypes of *Acinetobacter* baumannii isolated from patients in three hospitals in southern Vietnam. J Med Microbiol. 2017;66(1):46–53.
16. Strateva T, Sirakov I, Stoeva T, et al. Carbapenem-resistant *Acinetobacter* baumannii: current status of the problem in four Bulgarian university hospitals (2014–2016). J Glob Antimicrob Resist. 2019;16:266–73.
17. Rabin N, Zheng Y, Opoku-Temeng C, et al. Biofilm formation mechanisms and targets for developing antibiofilm agents. Future Med Chem. 2015;7(4):493–512.
18. Jiang X, Stockwell BR, Conrad M. Ferroptosis: mechanisms, biology and role in disease. Nat Rev Mol Cell Biol. 2021;22(4):266–82.
19. Tang D, Chen X, Kang R, et al. Ferroptosis: molecular mechanisms and health implications. Cell Res. 2021;31(2):107–25.
20. Deng L, He S, Guo N, et al. Molecular mechanisms of ferroptosis and relevance to inflammation. Inflamm Res. 2023;72(2):281–99.

Publisher's note

Springer Nature remains neutral with regard to jurisdictional claims in published maps and institutional affiliations.